10Gbit/s all-optical NRZ-OOK to RZ-OOK format conversion in an ultra-small III-V-on-silicon microdisk fabricated in a CMOS pilot line

Rajesh Kumar,[1, 2,*] Thijs Spuesens,[1,2] Pauline Mechet,[1,2] Nicolas Olivier,[3] Jean-Marc Fedeli,[3] Philippe Regreny,[4] Gunther Roelkens,[1,2] Dries van Thourhout,[1,2] and Geert Morthier[1,2]

[1]*Photonics Research Group, INTEC Department, Ghent University-IMEC, Sint-Pietersnieuwstraat 41, 9000 Ghent, Belgium*
[2]*Center for Nano- and Biophotonics (NB-Photonics), Ghent University, 9000 Ghent, Belgium*
[3]*CEA-LETI, Minatec Campus, 17 Rue des Martyrs, 38054 Grenoble, France*
[4]*Université de Lyon, Institut des Nanotechnologies de Lyon INL-UMR5270, CNRS, Ecole Centrale de Lyon, Ecully, F-69134, France*
[*]Rajesh.Kumar@intec.ugent.be

Abstract: We report the demonstration of an all-optical, bias free and error-free (bit-error-rate $\sim 10^{-12}$), 10Gbit/s non-return-to-zero (NRZ) to return-to-zero (RZ) data format conversion using a 7.5µm diameter III-V-on-silicon microdisk resonator. The device is completely processed in a 200mm CMOS pilot line. The data format conversion is based on the phenomenon of pulse carving of an NRZ optical data stream by an optical clock. The underlying physical effect for the pulse carving is the change in the refractive index caused by the generation of free-carriers in a pump –probe configuration. We believe it to be the first NRZ-to-RZ format convertor built on a hybrid III-V-on-silicon technology platform.

OCIS codes: (130.0130) Integrated optics; (130.3120) Integrated optics devices; (230.0230) Optical devices; (230.1150) All-optical devices; (230.5750) Resonators.

References and links

1. D. Norte, E. Park, and A. E. Willner, "All-optical TDM-to-WDM data format conversion in a dynamically reconfigurable WDM network," IEEE Photon. Technol. Lett. **7**(8), 920–922 (1995).
2. D. Breuer and K. Petermann, "Comparison of NRZ- and RZ-modulation format for 40-Gb/s TDM standard fiber systems," IEEE Photon. Technol. Lett. **9**(3), 398–400 (1997).
3. W. Astar, J. B. Driscoll, X. Liu, J. I. Dadap, W. M. J. Green, Y. A. Vlasov, G. M. Carter, and R. M. Osgood, Jr., "Conversion of 10 Gb/s NRZ-OOK to RZ-OOK utilizing XPM in a Si nanowire," Opt. Express **17**(15), 12987–12999 (2009), http://www.opticsinfobase.org/oe/abstract.cfm?uri=oe-17-15-12987.
4. L.-S. Yan, A.-L. Yi, W. Pan, B. Luo, and J. Ye, "Simultaneous NRZ-to-RZ format conversion and one-to-six error-free channel multicasting using a single pump in a highly nonlinear fiber," Opt. Express **18**(20), 21404–21409 (2010), http://www.opticsinfobase.org/abstract.cfm?URI=oe-18-20-21404.
5. X. Yang, A. K. Mishra, R. J. Manning, R. P. Webb, and A. D. Ellis, "All-optical 42.6Gbit/s NRZ to RZ format conversion by cross-phase modulation in a single SOA," Electron. Lett. **43**(16), 890–892 (2007).
6. X. Yang, A. K. Mishra, R. J. Manning, and R. Giller, "All-optical 40 Gbit/s NRZ to RZ format conversion by nonlinear polarization rotation in SOAs," Electron. Lett. **43**(8), 469–471 (2007).
7. J. Dong, X. Zhang, F. Wang, Y. Yu, and D. Huang, "Single-to-dual channel NRZ-to-RZ format conversion by four-wave mixing in single semiconductor optical amplifier," Electron. Lett. **44**(12), 763–764 (2008).
8. X. Zhao and C. Lou, "Investigation of all-optical nonreturn-to-zero-to-return-to-zero format converter based on a semiconductor optical amplifier and a reconfigurable delayed interferometer," Appl. Opt. **49**(7), 1158–1162 (2010).
9. J. Dong, X. Zhang, J. Xu, D. Huang, S. Fu, and P. Shum, "40 Gb/s all-optical NRZ to RZ format conversion using single SOA assisted by optical bandpass filter," Opt. Express **15**(6), 2907–2914 (2007), http://www.opticsinfobase.org/oe/abstract.cfm?URI=oe-15-6-2907.
10. . Nguyen Tan, M. Matsuura, and N. Kishi, "Transmission performance of a wavelength and NRZ-to-RZ format conversion with pulsewidth tunability by combination of SOA- and fiber-based switches," Opt. Express **16**(23), 19063–19071 (2008), http://www.opticsinfobase.org/oe/abstract.cfm?URI=oe-16-23-19063.
11. C. G. Lee, Y. J. Kim, C. S. Park, H. J. Lee, and C.-S. Park, "Experimental demonstration of 10-Gb/s data format conversion between NRZ and RZ using SOA-loop-mirror," J. Lightwave Technol. **23**(2), 834–841 (2005).

12. S. Fu, W.-D. Zhong, P. P. Shum, and Y. J. Wen, "All-optical NRZ-OOK-to-RZ-OOK format conversion with tunable duty cycles using nonlinear polarization rotation of a semiconductor optical amplifier," Opt. Commun. **282**(11), 2143–2146 (2009).
13. G.-R. Lin, K.-C. Yu, and Y.-C. Chang, "10Gbit/s all-optical non-return to zero-return-to-zero data format conversion on a backward dark-optical-comb injected semiconductor optical amplifier," Opt. Lett. **31**(10), 1376–1378 (2006).
14. J. Yu, G. K. Chang, J. Barry, and Y. Su, "40Gbit/s signal format conversion from NRZ to RZ using a Mach-Zehnder delay interferometer," Opt. Commun. **248**(4-6), 419–422 (2005).
15. T. Kurosu, S. Namiki, R. Akimoto, H. Kuwatsuka, S. Sekiguchi, N. Yasuoka, K. Morito, T. Hasama, and H. Ishikawa, "Demonstration of 172-Gb/s optical time domain multiplexing and demultiplexing using integrable semiconductor devices," IEEE Photon. Technol. Lett. **22**(19), 1416–1418 (2010).
16. P. Apiratikul, W. Astar, G. M. Carter, and T. E. Murphy, "10-Gb/s wavelength and pulse format conversion using four-wave mixing in a GaAs waveguide," IEEE Photon. Technol. Lett. **22**(12), 872–874 (2010).
17. S. Pan and J. Yao, "Optical NRZ to RZ format conversion based on a frequency-doubling optoelectronic oscillator," in *Proceedings of IEEE LEOS annual meeting*(Institute of Electrical and Electronics Engineers, 2009), pp. 797–798.
18. X. Zhao, C. Lou, H. Zhou, D. Lu, and L. Huo, "Optical regenerative NRZ to RZ format conversion based on cascaded lithium niobate modulators," Opt. Express **18**(23), 23657–23663 (2010), http://www.opticsinfobase.org/abstract.cfm?URI=oe-18-23-23657.
19. L. Huo, Y. Dong, C. Lou, and Y. Gao, "Clock extraction using an optoelectronic oscillator from high-speed NRZ signal and NRZ-to-RZ format transformation," IEEE Photon. Technol. Lett. **15**(7), 981–983 (2003).
20. Y. Yu, X. Zhang, J. B. Rosas-Fernández, D. Huang, R. V. Penty, and I. H. White, "Simultaneous multiple DWDM channel NRZ-to-RZ regenerative format conversion at 10 and 20 Gb/s," Opt. Express **17**(5), 3964–3969 (2009), http://www.opticsinfobase.org/oe/abstract.cfm?URI=oe-17-5-3964.
21. G. Lu, L. Chen, and C. Chan, Novel NRZ-to-RZ Format Conversion with Tunable Pulsewidth Using Phase Modulator and Interleaver," in *Optical Fiber Communication Conference and Exposition and The National Fiber Optic Engineers Conference*, Technical Digest (CD) (Optical Society of America, 2006), paper JThB32, *http://www.opticsinfobase.org/abstract.cfm?URI=OFC-2006-JThB32*.
22. J. Wang, J. Sun, Q. Sun, X. Zhang, D. Huang, and M. M. Fezer, "First demonstration of PPLN +RSOA-based tunable all-optical NRZ-to-RZ format conversion," in *Proceedings of European Conference on Optical Communication* (2007), pp.: 1–2.
23. B. Li, M. I. Memon, G. Mezosi, Z. Wang, M. Sorel, and S. Yu, "All-optical logic gates using bistable semiconductor ring lasers," J. Opt. Commun. **30**(4), 190–194 (2009).
24. Data sheet CIP SOA(SOA-L-OEC-1550), *http://www.coretk.com/CataLog/cata_img/FILE/963076829/CIP/166_167_1139895559.pdf*
25. T. Spuesens, D. Van Thourhout, P. Rojo-Romeo, P. Regreny, and J.-M. Fedeli, "CW operation of III-V microdisk lasers on SOI fabricated in a 200 mm CMOS pilot line," in *Proceedings of Group IV photonics* (2011), pp: 199–201.
26. M. Kostrzewa, L. Di Cioccio, J. M. Fedeli, M. Zussy, P. Regreny, J. C. Roussin, and N. Kernevez, "Die-to-Wafer molecular bonding for optical interconnects and packaging," EMPC, Brugge, Belgium, June 12–15, 2005.
27. V. Van, T. A. Ibrahim, P. P. Absil, F. G. Johnson, R. Grover, and P.-T. Ho, "Optical signal processing using nonlinear semiconductor microring resonators," IEEE J. Sel. Top. Quantum Electron. **8**(3), 705–713 (2002).
28. R. Kumar, T. Spuesens, P. Mechet, P. Kumar, O. Raz, N. Olivier, J.-M. Fedeli, G. Roelkens, R. Baets, D. Van Thourhout, and G. Morthier, "Ultrafast and bias-free all-optical wavelength conversion using III-V-on-silicon technology," Opt. Lett. **36**(13), 2450–2452 (2011).
29. D. Liang and J. E. Bowers, "Recent progress in lasers on silicon," Nat. Photonics **4**(8), 511–517 (2010).
30. L. Liu, R. Kumar, K. Huybrechts, T. Spuesens, G. Roelkens, E.-J. Geluk, T. de Vries, P. Regreny, D. Van Thourhout, R. Baets, and G. Morthier, "An ultra-small, low-power, all-optical flip-flop memory on a silicon chip," Nat. Photonics **4**(3), 182–187 (2010).
31. S. F. Preble, Q. Xu, B. S. Schmidt, and M. Lipson, "Ultrafast all-optical modulation on a silicon chip," Opt. Lett. **30**(21), 2891–2893 (2005).
32. G. P. Agrawal, *Fiber-Optic Communication Systems* (John Wiley & Sons, 2002), Chap. 4.

1. Introduction

Return-to-zero (RZ) and non-return-to-zero (NRZ) are the modulation formats that are commonly used in optical communication systems. Depending upon the size and requirements of the network, either the NRZ or RZ modulation format can be selected for use in future optical networks [1]. The RZ data format is widely employed in optical time-division multiplexing (OTDM) systems due to its tolerance for polarization mode dispersion and fiber nonlinearities [2]. The NRZ format is preferred in wavelength division multiplexed (WDM) networks owing to its high spectral efficiency and tolerance to timing-jitter. Format conversion from NRZ to RZ and vice-versa becomes important to add to the flexibility and scalability of optical networks. To perform the format conversion from NRZ to RZ all-optical e.g [3–16] as well as optoelectronic e.g [17–21] approaches have been explored. Most of the

investigated all-optical approaches employed semiconductor optical amplifiers (SOAs) and very few used other devices such as periodically poled lithium niobate waveguides [22], silicon waveguides [3], III-V waveguides [16] and III-V ring lasers [23]. All-optical data format conversion devices based on SOAs have a large footprint with the cavity length of a single SOA varying from several hundreds of micrometers to a few tens of millimeters, e.g. the SOA used in reference [12] has a cavity length of 20.83 mm [24]. Moreover the SOA based format convertors need a DC bias of several hundreds of mAs which results into extra power consumption. Likewise other kinds of format converters [3,16–23] have large footprints which reduce their potential for compact integration and make them less suitable for practical applications. In the past decade there has been an intensive focus on the use of the silicon-on-insulator (SOI) platform for the fabrication of photonic devices due to its CMOS compatibility. All-optical devices fabricated in pure silicon rely on nonlinear effects such as four-wave-mixing (FWM), self-phase modulation (SPM), and two photon absorption (TPA) etc. but these effects in silicon are known to be power-hungry. The NRZ to RZ format conversion has been shown to be viable [3] on a silicon chip using a 5mm long silicon waveguide in pump-probe configuration but the total average power used was quite high (~34dBm in the silicon waveguide). Power consumption can be reduced in III-V-on-silicon resonating structures (such as microdisks and microrings) along with the reduction in the footprint of the device while still taking the advantage of CMOS fabrication processes [25,26] and maintaining the high speed of operation by exploiting the plasma dispersion effect resulting from the free carrier generation in a pump-probe configuration. In III-V material based resonating structures the carrier recovery time of tens of picoseconds has already been demonstrated [27,28]. Several heterogeneous III-V/silicon devices have already been demonstrated such as lasers [29] and all-optical flip-flops [30], and the integration of all these functionalities on a single chip is within reach. In this paper we present the demonstration of an all-optical 10Gbit/s NRZ-OOK to RZ-OOK format conversion, without using any dc electric bias, in an InP-InGaAsP disk of 7.5 micron diameter heterogeneously integrated on top of an SOI waveguide circuit. The fabrication of the silicon chip having several of these InP-InGaAsP microdisk/microring, race-track resonators and photodetectors is carried out in a 200mm CMOS pilot line.

2. Device design and resonance characteristics

The SOI waveguide circuit is defined using 193nm deep ultra-violet (DUV) lithography. The width and the thickness of the silicon waveguide is 600nm and 220nm respectively, while the BOX (buried oxide) is 2µm thin. Grating couplers are used to couple light in- and out of the SOI waveguide. The III-V material is bonded on top of the SOI waveguide circuit using a SiO_2 molecular bonding process resulting into a 130nm thick bonding layer. The III-V microdisk is etched such that the periphery of the microdisk overlaps with the silicon waveguide covering a width of 500nm. This overlapping section allows the evanescent coupling of the light from the waveguide to the microdisk and vice-versa. The active region of the microdisk structure contains three compressively strained InAsP quantum wells each of them being 6 nm thick. The total thickness of the microdisk is ~580nm. More details on the design as well as on the fabrication process can be found in ref [25]. The transmission resonance characteristics of the microdisk resonator are found by scanning the wavelength of a continuous wave (CW) tunable laser and the normalized transmission response of the microdisk as a function of wavelength is plotted in Fig. 1. As can be seen from the figure, there exist two azimuthal mode resonances separated by an FSR (free spectral range) of 30.8nm. The photon life time of the resonator at resonances 1550.1nm and 1580.1nm is 1.77ps and 3.32ps is respectively. It is observed that the dependence of the photon life time on the optical power is negligibly small. There are also other resonances which correspond to higher order radial modes and have a low extinction ratio as compared to that of the azimuthal modes. In addition, some ripples are also visible in the transmission spectrum.
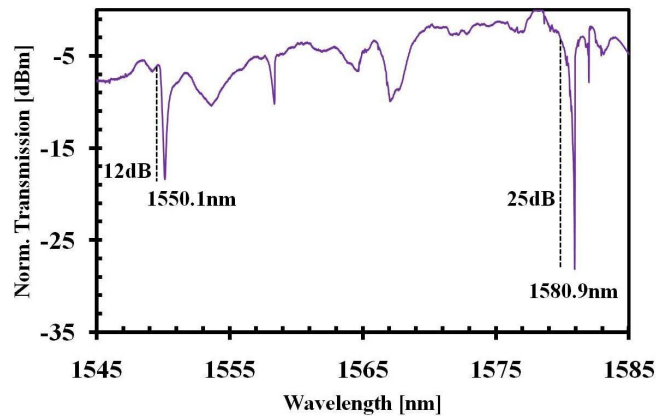
Fig. 1. Transmission response of the microdisk resonator.

They are due to a Fabry-Perot resonance formed between the grating couplers at each end of the silicon waveguide used for in- and out-coupling of light through single mode fiber, and reflections from the fiber-facets, connectors etc. For in- and out-coupling of the light, the fiber-to-fiber loss is 12dB. The intrinsic loss of the resonator is found to be 40dBcm^{-1} while the propagation loss of the SOI waveguide is 2dBcm^{-1}. The extinction ratio of the lower wavelength (~12dB: 1550.1nm) resonance is less than that of the higher wavelength (~25dB: 1580.9nm) resonance. This is due to the fact that the higher wavelength resonance lies closer to the band-gap wavelength of the active material and hence has less absorption in comparison to the lower wavelength resonance.

3. Concept of NRZ to RZ format conversion

Using the effect of refractive index modulation caused by the free carrier generation in a pump-probe configuration, the transmission characteristics of the microdisk/ring resonators can be changed in real-time [27,31]. In the pump-probe configuration, a probe is tuned to one resonance wavelength while the pump is tuned to another. If an optical pulse train (clock, here after) is used as a pump and the data signal as a probe, then the pattern as well the format of the data signal can be changed. If the wavelength of the data signal is chosen to be on-resonance then in the absence of the clock pulses, the data signal will be coupled into the microdisk. In the presence of the clock pulses, free carriers will be generated resulting in a blue shift of the resonance and the data will become off-resonance for the duration of the pulses. This way the data output from the microdisk will be high or low depending upon the presence or absence of the clock pulses. If the clock pulse duration is shorter than the bit duration of the data then the format of the NRZ signal becomes RZ. Figure 2 illustrates the concept by taking an example of data pattern and clock signal. In Fig. 2(a) the clock pulse duration is chosen equal to the bit duration. If the data pattern 0000111100001111…..is imprinted on a resonance wavelength of the microdisk, then only for the duration for which the clock as well as the input data is high, the output data will be high. Therefore, the data pattern at the output becomes 0000010100000101….If we consider the consecutive four 1s to be a single pulse; we can say it has been carved into two smaller pulses. As illustrated in Fig. 2(b), if the duration of the clock pulse is less than that of a bit and both the clock as well as data are high, in the output each '1'occupies the time of the clock pulse. This is effectively the conversion of the data format from NRZ to RZ.
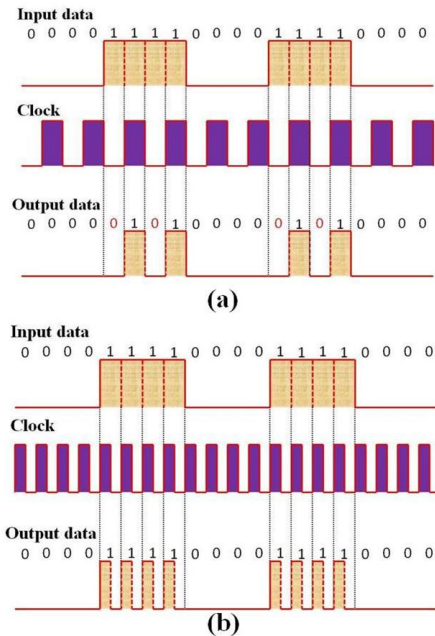
Fig. 2. Illustration of (a) data output as a function of level (high /low) of the clock, (b) format conversion from NRZ to RZ.

4. Experiments and results

Experiments are done first to verify the concept of pulse carving, as illustrated in Fig. 2(a), using a 10Gbit/s NRZ-OOK signal and 5GHz clock. The schematic of the experimental set-up used is shown in Fig. 3. Using a pulse pattern generator (PPG), a 10Gbit/s NRZ electrical data pattern of four consecutive 1s followed by four consecutive 0s, and there after repeating periodically, is generated. The electrical data pattern is converted into the optical domain by using the first electro-optic LiNbO3 modulator (MOD1) and the first tunable laser (TL1). Use of polarization controlling wheels (PCWs) ensures that the generated optical data is TE polarized. Using the ½ clock output of the PPG, a second electro-optic LiNbO3 modulator (MOD2) and the second tunable laser (TL2); an optical clock with a repetition rate of 5GHz is generated. The tunable lasers TL1 and TL2 are tuned to the resonant wavelengths 1580.9nm and 1550.1nm respectively. Output of the MOD2 is amplified using a C band erbium-doped fiber amplifier (EDFA1) and is followed by an optical delay line to synchronize the optical clock with the optical input data. The output data is collected at the drop-port of an optical circulator (OC) and is amplified using an L band erbium-doped fiber amplifier (EDFA2). An optical band pass filter (OBPF) follows the EDFA2 to suppress the ASE noise. A variable optical attenuator (VOA) is used to control the input power to the high-speed photodiode (HSPD) connected to the scope. The waveform of the optical data and the optical clock is shown in Fig. 4(a) and 4(b) respectively. The average power of the input optical data and the optical clock in the SOI waveguide is estimated to be ~-2 and + 1 dBm respectively. In the absence of the optical clock, the optical data signal remains coupled into the microdisk and a low power level is seen on the scope. Injection of the optical clock pulses into the microdisk results into the generation of the free carriers causing a blue-shift of the resonance. This
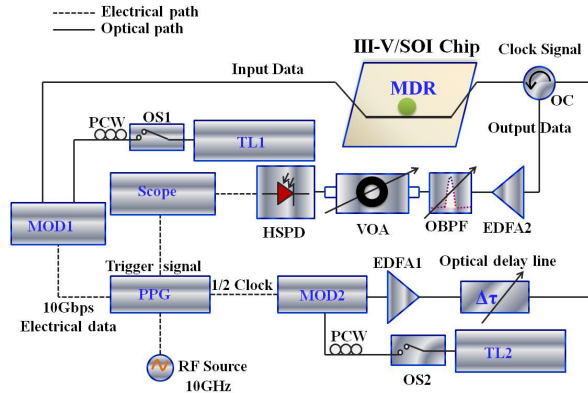
Fig. 3. Schematic of the experimental setup for pulse carving measurements. OS: Optical Switch, MDR: Microdisk Resonator.
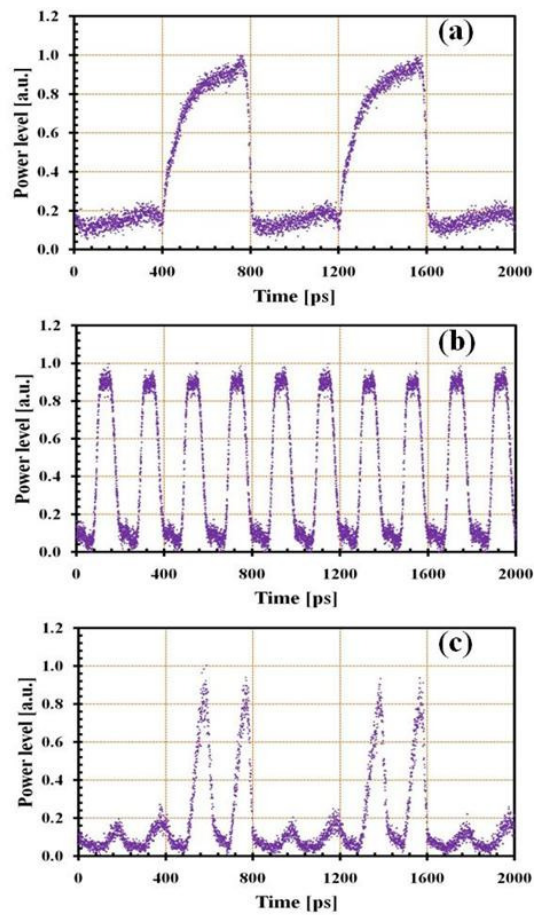

Fig. 4. Waveform of (a) optical input data, (b) optical clock and (c) optical output data.

causes the input optical data to go out of resonance. Therefore, output optical data has a high power level only when both the input optical data as well as the optical clock are high as illustrated in Fig. 4(c). It is clear from these plots that a 400ps input data pulse, which is

formed as a result of four consecutive 1s, has been divided into two pulses and first and third 1s have been converted to 0s due to the low level of the optical clock in this time interval. This way the data pattern has changed from 0000111100001111…..to 0000010100000101…..as discussed in section 3. Secondly, by choosing the clock pulses shorter than the bit duration, format conversion experiments are performed and the system performance in terms of the bit-error-rate and Q factor of the eye diagrams is evaluated. The sketch of the experimental set-up used for this purpose is drawn in Fig. 5. The method of generating the optical input data remains the same as in the first experiment. To generate the optical clock signal, a short pulse source (SPS) is used. It is driven by the same RF source, using a 3dB RF splitter, which drives the PPG. The optical clock at 10GHz has a pulse width (FWHM) of ~8ps. A variable optical attenuator (VOA1) is used to regulate the output power of the optical clock. The procedure of detecting the optical output data is the same as in the first part. For the bit-error-rate measurements, the electrical output data from the scope is fed to a bit-error-rate tester (BERT). First a 10Gbit/s NRZ-OOK optical input data pattern of alternate 1s and 0s is used.
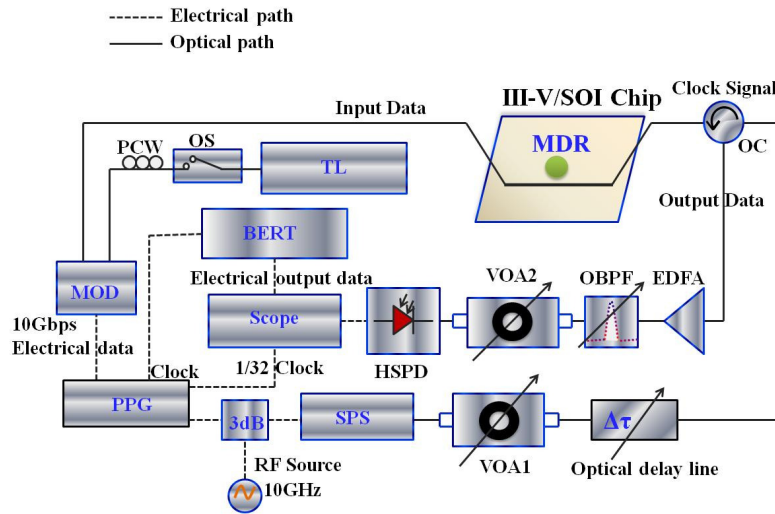

Fig. 5. Schematic of the experimental set-up used for the format conversion. OS: Optical Switch, MDR: Microdisk Resonator

The input optical data waveform consisting of alternate 1s and 0s and the optical clock is shown in Fig. 6(a) and 6(b) respectively. In Fig. 6(b), the pulse width looks much wider than its actual width (FWHM~8ps) due to the limited bandwidth of the photodiode (~30GHz). Figure 6(c) shows the format converted optical data output pattern. The 1 bit of the optical output data occupies a time slot of ~50ps although the clock duration is much shorter than this time slot. This is due to the slower dynamics of the photo-generated carriers in the microdisk. For the system performance measurements, the optical input data signal is changed to a PRBS pattern of length 2^7-1. Figure 7(a) shows a part of the waveform of the format converted PRBS signal from NRZ to RZ. Figure 7(b) shows the bit-error measurement curves of the input NRZ and the output RZ data. It is to be noted that the BER measurements for the input NRZ data is performed by keeping it off-resonance of the microdisk. An error free (BER~10^{-12}) format conversion is achieved with a power penalty of 3.6 dB. The ASE noise added due to the amplification of the format converted signal results into the power penalty. The patterning effect is another possible source of signal degradation and the power penalty.
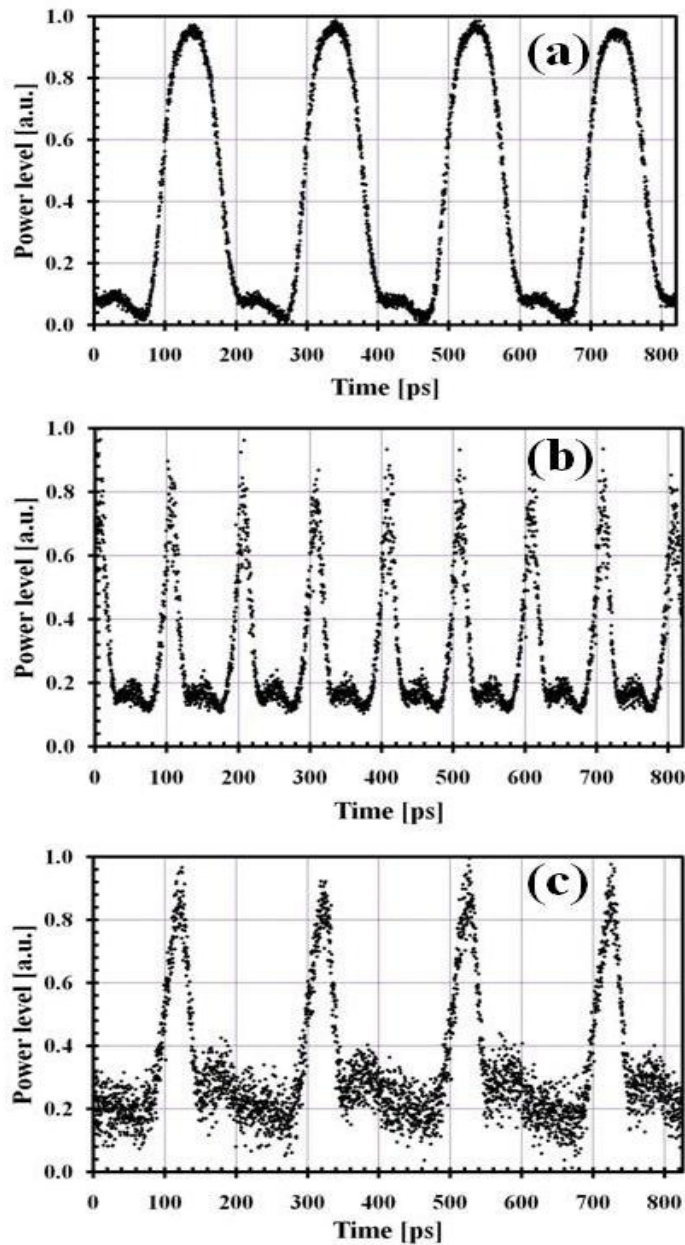
Fig. 6. Waveform of (a) optical input data, (b) optical clock and (c) optical output data.

The amplification is required for the format converted signal because it has half the power of the original signal due to the basic procedure and principle of the format conversion involved here. We also compared the Q factor and the BER at different received powers. It is found that the Q factor matches very well to the measured BER. For example, at a received power of ~-6dBm, the Q factor is ~6 which correspond to a BER ~10^{-9} [32] and the same is found from the BER measurements as can be seen from Fig. 7(b). As an illustration, the eye diagram of the format converted signal and that of the original signal is shown in Fig. 7(b).
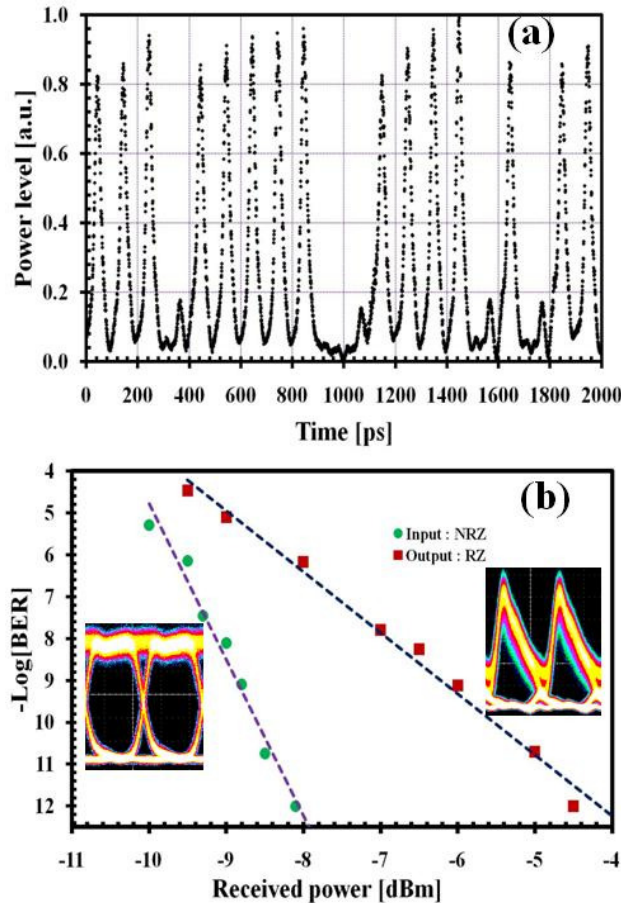
Fig. 7. (a) Waveform of a part of the format converted PRBS data and (b) System performance: BER and eye diagram before (left) and after (right) format conversion. The time scale for both the eye diagrams is 48ps/division.

5. Discussion and conclusions

Although a lot of work has been done on the microdisk/ring based devices but for their real applications, further investigations and improvements are needed and the same is true about the format convertor presented here. The bandwidth of the microdisk/ring resonators is quite narrow and for wide band applications an array of the microdisks of varying diameters can be used. Microdisk/ring based resonators are temperature sensitive and this problem can be removed by making them athermal using the coating of the polymers which have the thermo-optic coefficient opposite to that of the resonators.

In conclusion, we have demonstrated an error free 10Gbit/s NRZ-OOK to RZ-OOK format conversion in a small III-V-on-silicon microdisk completely processed in a CMOS pilot line. The format conversion is achieved with a moderate power penalty and relatively low average power consumption in a pump-probe configuration. The wavelength of the data signal remains preserved after the format conversion. The speed of the format conversion can be further increased by (a) applying a reverse bias, (b) use of a holding beam, and (c) ion-implantation in the active region of the microdisk resonator to improve the carrier dynamics. The demonstrated format convertor has a small foot-print; therefore, it has the potential of integration with other active and passive on-chip devices.

Acknowledgments